Available online at www.sciencedirect.com
SCIENCE DIRECT
Catalysis Today 104 (2005) 352–359
CATALYSIS TODAY
www.elsevier.com/locate/cattod

On the combination of different transport mechanisms for the simulation of steady-state mass transfer through composite systems using H_2/SF_6 permeation through stainless steel supported silicalite-1 membranes as a model system

M. Hanebuth [a], R. Dittmeyer [a,*], G.T. P. Mabande [b], W. Schwieger [b]

[a] *DECHEMA e.V., Karl-Winnacker-Institut, Theodor-Heuss-Allee 25, D-60486 Frankfurt am Main, Germany*
[b] *Friedrich-Alexander-Universität Erlangen-Nürnberg, Lehrstuhl für Chemische Reaktionstechnik, Egerlandstr. 3, D-91058 Erlangen, Germany*

Available online 11 April 2005

Abstract

A method to calculate the steady-state multicomponent mass transfer in heterogeneous structures is presented. For this, different transport mechanisms represent different regions inside the composite system. The solving scheme allows the calculation of the molar flow rates along the different transport pathways and the estimation of unknown transport parameters based on experimental data.

The steady-state mass transfer of hydrogen and sulfur hexafluoride through a sinter metal supported MFI zeolite membrane is examined as a model system. The support is simulated using the dusty gas model, the molecules passing the zeolite layer may follow transport mechanisms like Knudsen diffusion, surface diffusion or activated gas diffusion. The configuration used, with data from single gas experiments, can predict the binary system only at high temperatures. The problems arising at low temperatures are due to the oversimplified assumption that adsorbed and desorbed molecules do not interact on their way through the MFI zeolite micropores.

However, because of the modular structure of the approach, it can be easily extended to more advanced transport models to account for interactions between the different molecules. And the method can be applied equally well to other systems, such as palladium composite membranes or membranes with catalytic activity.

Keywords: Composite membrane; Zeolite membrane; MFI; Gas separation; Hydrogen; Sulfur hexafluoride; Simulation

1. Introduction

For the simulation of membrane reactors it is necessary to calculate the multi component mass transfer through composite membranes. Often this is done with transport models assuming a homogeneous structure, while the resistance of the support layer is not taken into account. In addition to the influence of the support, often defects of the selective layer must not be neglected since they can reduce the separation selectivity of a membrane drastically. There is a lack of attention to this problem in literature; most articles do not tackle it in a quantitative manner. But there are some exceptions.

For example, in [1] the mass transport through hydrogen selective palladium membranes is simulated, while the influence of the support and that of defects in the palladium layer are considered. There are some other examples dealing with polycrystalline MFI type zeolite membranes: in [2] the porosity of the support is used to account for the decreased area of the available zeolite layer. A binary diffusion model for the porous support is applied in [3,4], and in [5] the influence of the support is calculated with the dusty gas model. In [6] the authors discuss a method to estimate the part of membrane transport taking place through defects and in [7], for the case of single gas permeation, the zeolitic pores and defects are treated separately.

Dividing a composite membrane into different regions with corresponding transport mechanisms is a typical approach in simulating the mass transfer. For this, the

* Corresponding author. Tel.: +49 69 7564 428; fax: +49 69 7564 388.
E-mail address: dittmeyer@dechema.de (R. Dittmeyer).

0920-5861/$ – see front matter © 2005 Elsevier B.V. All rights reserved.
doi:10.1016/j.cattod.2005.03.057

a	model parameters
A	area (m^2)
B_0	parameter for dusty gas model (m^2)
c	concentration (mol m^{-3})
D	diffusion coefficient (m^2 s^{-1})
$\mathcal{D}$	diffusion coefficient (Maxwell and Stefan) (m^2 s^{-1})
E_A	activation energy (J mol^{-1})
J	flux (mol m^{-2} s^{-1})
K_0	parameter for dusty gas model (m)
M	mass of molecule (kg mol^{-1})
n	number of components (1)
$\dot{n}$	molar flow (mol s^{-1})
N	number of data points (1)
p	pressure (Pa)
q	loading (mol kg^{-1})
R	gas constant (J mol^{-1} K^{-1})
T	temperature (K)
x	mole fraction (1)
x	independent variables
z	probability factor (1)

Greek letters

Γ	thermodynamic factor (1)
δ	length of transport path (m)
ε	porosity (1)
η	viscosity (Pa s)
λ	jump length (m)
μ	chemical potential (J mol^{-1})
π	3.14159 (1)
ρ	Density (kg m^{-3})
σ	variance
τ	tortuosity (1)

Subscripts

GT	gas translation
i	component in mixture
j	component in mixture
k	index of transport path
K	Knudsen diffusion

Superscripts

e	effective
EXP	experiment
sat	saturation
SIM	simulation

partial pressures at some points inside the composite membrane must be calculated balancing the mass transport. The resulting equations have to be solved simultaneously with the transport equations to obtain the resulting mass flows for the whole membrane. But these equations become rather complicated for multicomponent systems, because the interactions between the different species call for sophisticated models. Furthermore, for multicomponent systems and for complicated membrane structures the number of equations increases drastically. As a result, it is only possible for simple systems to solve these equations by hand.

In this paper we present a method to overcome these limitations. The algorithm that solves the equations iteratively is the same for every system and membrane configuration. Established transport models, like the dusty gas model, (activated) Knudsen diffusion or surface diffusion are employed as transport paths which can be combined to simulate heterogeneous structures. The model can also be extended by including other transport mechanisms or by assigning catalytic activity to certain transport paths. This approach is demonstrated here first using the example of hydrogen and sulfur hexafluoride single gas transport through a polycrystalline MFI zeolite membrane supported by a porous sinter metal disk, as sketched in Fig. 1. Later on the binary transport behavior of this system is analyzed using the transport parameters derived from the unary experiments.

2. Mathematical model

Before different transport mechanisms are combined, a brief summary of the most common mechanisms occurring inside composite membranes shall be given.

2.1. Dusty gas model

The transport resistance of the porous support can be calculated according to the dusty gas model [8,9].

$$\nabla x_i = \frac{RT}{p}\left[\sum_{j=1}^{n}\frac{\mathbf{J}_j x_i - \mathbf{J}_i x_j}{(\varepsilon/\tau)\,D_{i,j}} - \frac{\mathbf{J}_i}{D^{e}_{i,K}}\right] - x_i\left(\frac{1}{p} + \frac{B_0}{\eta D^{e}_{i,K}}\right)\nabla p \tag{1}$$

The index $i = 1, \ldots, n$ marks different species. Three different transport mechanisms are included in this equation. Each has its own geometry parameter: molecular diffusion occurs in large pores for multi-component systems and is influenced by the factor ε/τ, accounting for porosity and tortuosity of the pores. For viscous flow, there is the parameter B_0. For the last transport mechanism of the dusty gas model, Knudsen diffusion, one has the parameter K_0, which is related to the effective Knudsen diffusion coefficient:

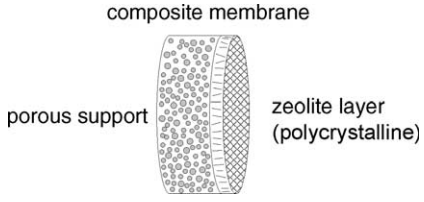

Fig. 1. Schematic view of a composite membrane.

$$D^{e}_{i,K} = \frac{4}{3} K_0 \sqrt{\frac{8RT}{\pi M_i}} \tag{2}$$

The three parameters can be determined by rather simple experiments, using the uncoated porous support.

2.2. Activated Knudsen diffusion

Like in the support, also inside the zeolite layer different transport mechanisms can occur. Inside zeolite pores the passing molecules may be in adsorbed or desorbed state [10,3]. For desorbed molecules an activated analog of Knudsen diffusion is frequently assumed:

$$\mathbf{J}_{GT} = -D_{GT} \nabla c \tag{3}$$

$$D_{GT} = \frac{\lambda}{z} \sqrt{\frac{8RT}{\pi M}} \exp\left[-\frac{E_{A,GT}}{RT}\right] \tag{4}$$

2.3. Surface diffusion

The diffusion of adsorbed molecules can be calculated according to the Maxwell–Stefan formulation [11,12]. With the density of the zeolite denoted by ρ and the loading of component i designated by q_i, the equations become:

$$-\rho \frac{q_i}{q_i^{sat} RT} \nabla \mu_i = \sum_{j=1}^{n} \frac{q_j \mathbf{J}_i - q_i \mathbf{J}_j}{q_i^{sat} q_j^{sat} \mathcal{D}_{ij}} + \frac{\mathbf{J}_i}{q_i^{sat} \mathcal{D}_i}. \tag{5}$$

The second term on the right hand side stands for interactions of the molecules with the pore wall. The gradient of the chemical potential $\nabla \mu_i$ can be expressed in terms of a matrix of thermodynamic factors $[\Gamma]$:

$$\frac{q_i}{q_i^{sat} RT} \nabla \mu_i = \sum_{j=1}^{n} \frac{\Gamma_{ij}}{q_j^{sat}} \nabla q_j \tag{6}$$

The matrix $[\Gamma]$ can be calculated from the multicomponent adsorption isotherms, while multicomponent adsorption can be modelled according to the theory of ideal adsorbed solutions (IAS) [13–18].

$$\Gamma_{ij} = \frac{q_j^{sat}}{q_i^{sat}} \frac{q_i}{p_i} \frac{\partial p_i}{\partial q_j} \tag{7}$$

2.4. Knudsen diffusion

The intercrystalline regions of polycrystalline zeolite membranes can have a significant influence on the transport behavior. Depending on membrane quality, a certain number of mesoporous defects are always present in the zeolite layer. In such pores with enlarged diameter the molecules are likely to follow a Knudsen diffusion mechanism:

$$\mathbf{J}_i = -D_{iK} \nabla c_i \tag{8}$$

The diffusion coefficient D_K can be calculated from Eq. (2). For Knudsen diffusion the flux is proportional to the pore diameter, whereas it is proportional to the square of the pore diameter in case of viscous flow. This is the reason why in polycrystalline zeolite layers no significant contribution of viscous flow arises unless there are macroporous defects.

2.5. Combining different mechanisms

To deal with the structure of composite membranes, different transport pathways are connected at specific points inside the membrane, as shown in Fig. 2.

It is not practical to seek for analytical solutions for every possible configuration, since there is an infinite number of possible connection schemes that can describe the behavior of a composite system. It is much more pragmatic to look for a general numerical procedure. To calculate the fluxes along the different pathways, it is necessary to know the partial pressures at each connection node. Unfortunately, only the variables of the outer nodes can be determined by experiment. The partial pressures at the inner nodes must be calculated iteratively by balancing the molar flows.

$$\dot{n}_i = \mathbf{J}_i \cdot A \tag{9}$$

In steady state, each molecule entering an inner node leaves immediately through one of the other pathways connected to this node. With a good initial guess, the partial pressures at the inner nodes can therefore be determined by a Newton–Raphson algorithm [19].

Since there is no accumulation, the sum of the molar flows of each species i through all transport paths at an inner node must equal zero:

$$\sum_k \dot{n}_i = 0, \qquad i = 1, \ldots, n. \tag{10}$$

Another problem that arises is, that some parameters connected to certain transport paths are unknown (for example the area A in Eq. (9)). To find estimates for these parameters a second iteration is used: The total flux through the membrane is fitted to the experimental data using a Marquardt–Levenberg algorithm [19]. It minimizes the merit function χ^2 in adjusting the unknown parameters $\mathbf{a}$, while for

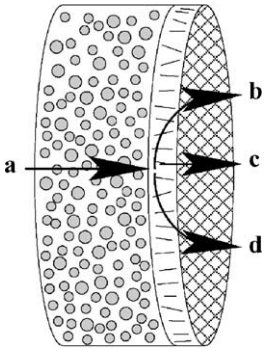

Fig. 2. A composite membrane can be regarded as connected pathways. In this example the support is modelled using the dusty gas model (a). The molecules can pass the zeolite layer via surface diffusion (b), in desorbed state following an activated gas diffusion mechanism (c), or through defects via Knudsen diffusion (d).

each change of these parameters a new convergence of the inner Newton–Raphson iteration (Eq. (10)) is needed:

$$\chi^2(\mathbf{a}) = \sum_{i=1}^{N} \left[\frac{\dot{n}_i - \dot{n}(\mathbf{x}_i, \mathbf{a})}{\sigma_i} \right]^2 \quad (11)$$

The independent variables $\mathbf{x}_i$ are the temperature and the partial pressures in the permeate and the retentate. Their values must be known from the experiment.

2.6. Implementation

The programming language C++ was used to implement the presented model. Fig. 3 shows the structure of the program.

Presently the dusty gas model, Knudsen diffusion with the possibility of an activation energy and surface diffusion are implemented, while the modular structure of the program allows other transport mechanisms to be added. The implementations for the Newton–Raphson and Marquardt–Levenberg algorithms were taken from [19].

3. Experimental

For steady-state permeation measurements with composite zeolite membranes the apparatus shown in Fig. 4 was used. It allows to determine the permeance of planar disk-shaped membranes with a diameter of 18 mm.

The upper and lower sides of the permeation cell are heated independently. Thereby the temperature difference between the two compartments during a measurement was kept below 1 K. To avoid as good as possible leakage out of the apparatus, in addition to the use of polymer O-ring gaskets the outside of the composite membrane was also sealed by an epoxy resin.

Single gas experiments were carried out in the following way: The used gas was passed at constant flow through the feed side by means of a thermal mass flow controller (Brooks), while a back pressure controller served to keep the pressure at 200 kPa. A soap bubble flow meter was used to quantify the permeating flux. Hence the permeate side pressure was slightly above ambient pressure (100 kPa). To measure the temperature dependency of the single gas permeance, the membranes were heated to 450 K for at least 8 h inside the apparatus under a flow of the respective gas on both sides of the membrane. During the experiments the heating- and cooling rate was set to 0.5 K/min to avoid thermal stress on the zeolite layer.

For multicomponent experiments the setup was slightly changed. The feed mixture was supplied with two thermal mass flow controllers at least. In addition to the volumetric flow rate measured by the soap bubble flow meter, the permeating gas was analyzed by a gas chromatograph to determine its composition. The experiments were performed without sweep gas because the objective was to have conditions comparable to the single gas experiments. This is

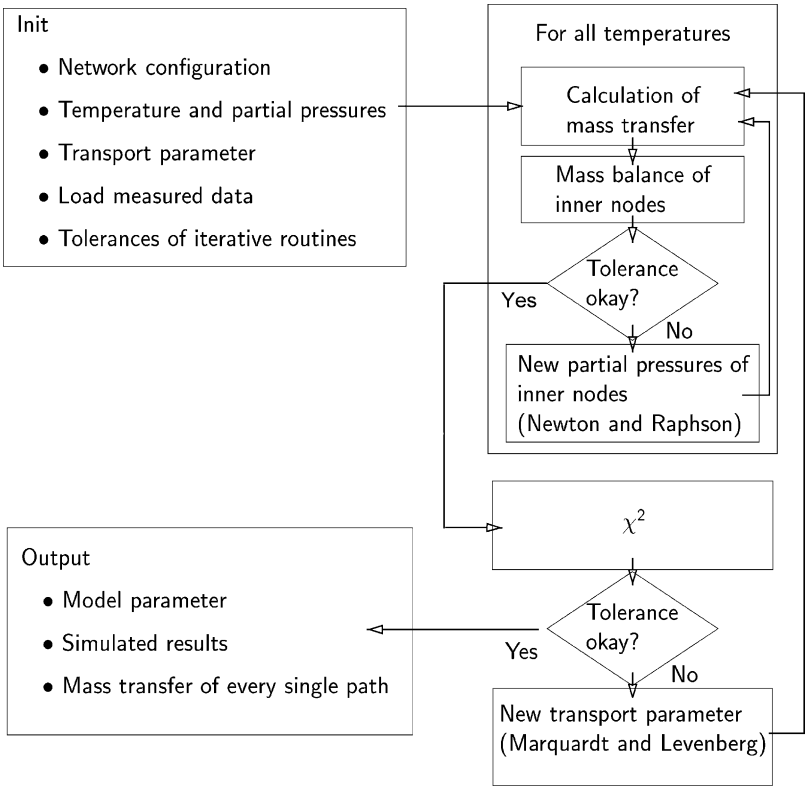

Fig. 3. The structure of the implemented program.

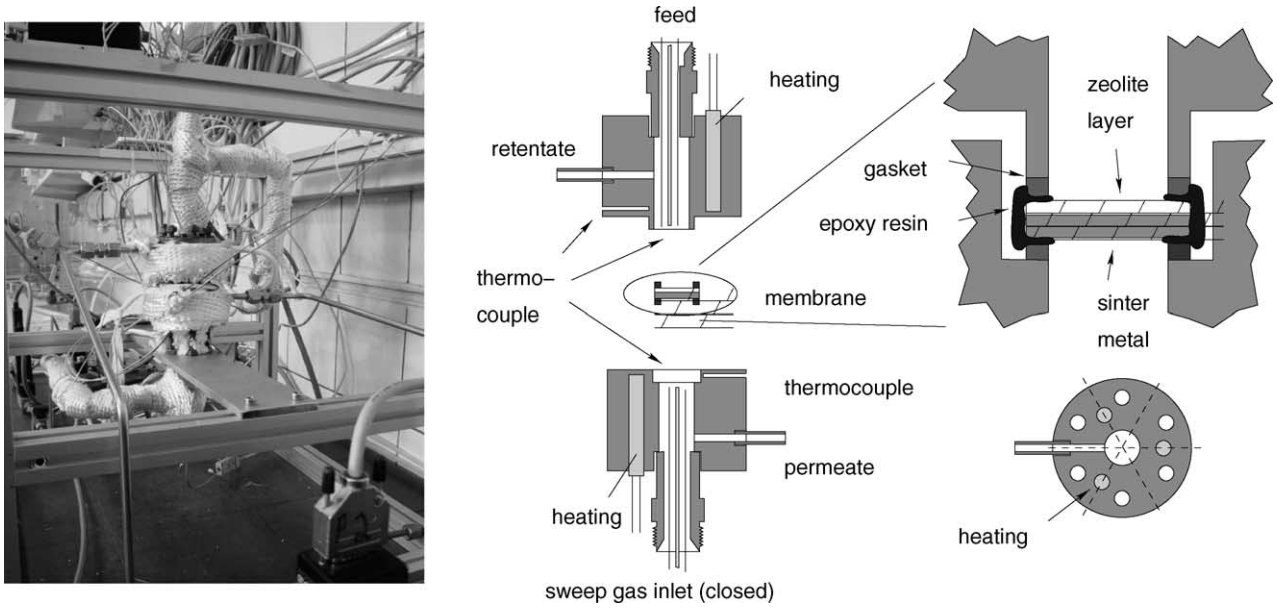

Fig. 4. Permeation cell for planar membranes.

also why on the retentate side the pressure was set again to 200 kPa while on the permeate side ambient pressure prevailed (100 kPa). Due to the relatively small membrane area the permeating flow was generally low. It took more than 30 min until the mixture had displaced the gas in the pipelines to the gas chromatograph and no further changes in its composition could be observed.

4. Gas permeation and simulation

The relatively new family of zeolite membranes can serve as an example for composite membranes. In our case a silicalite-1 membrane with a sinter metal support and a membrane thickness of about 20 μm was examined. The preparation was carried out via two hydrothermal synthesis steps. Details of the preparation method have been already described elsewhere [20,21] (Membrane 2).

Hydrogen and sulphur hexafluoride were used as representative model systems. While the non-adsorbing hydrogen has a very small kinetic diameter of 0.29 nm, the diameter of the bulky sulfur hexafluoride is comparable to the pore diameter of the MFI zeolite pores. This molecule also shows a stronger tendency to adsorb on the zeolite pore walls.

4.1. Hydrogen

To simulate the transport of hydrogen through a zeolite membrane, the first question that should be answered is: Which mechanism represents the true transport inside the zeolite pores best? In the literature there is no clear answer to this question. For example, in [22] hydrogen transport through an MFI zeolite membrane is modelled via surface diffusion, in [23] activated gas diffusion is assumed, while in [24] Knudsen diffusion is considered.

Adsorption isotherms for silicalite-1 powder [25] show that the adsorption of hydrogen is quite weak. It seems therefore unlikely that a large amount of the molecules would undergo a surface diffusion mechanism. Hence a mechanism for desorbed molecules should describe the membrane better. Regarding the ratio of the kinetic diameter to the pore diameter ($0.29\,\text{nm}/0.55\,\text{nm} \approx 0.53$), one can conclude that this diffusion process most likely is not activated. As a rule of thumb, activated diffusion starts to come into play at a ratio of the kinetic diameter versus the pore diameter in the range of 0.6–0.8 [10]. A pure Knudsen mechanism should therefore be most suitable for the transport of hydrogen through the zeolitic pores.

In the non-zeolitic pores the picture is quite similar. Since most of these pores (defects) are presumably larger than the zeolite pores, there should not be the need for an activation of gaseous molecules like hydrogen to pass. But typically, for reasonable membranes, the defects are not that large in size to allow for a significant contribution of viscous flow. Therefore, the resulting mechanism for the transport of hydrogen through non-zeolitic pores is Knudsen diffusion. This makes it difficult to distinguish between the amount of hydrogen permeating through the defects and that transported through the zeolite pores based on steady-state permeation data.

The influence of the porous support should not be very strong for unary systems because in that case there is no molecular diffusion. But since the dusty gas parameters were known from earlier experiments with nitrogen, this transport path was added to the used configuration as well. The dusty gas parameters for the used support (SIKA-F AS from GKN, Sinter Metal Filters GmbH, Radevormwald, Germany) are $B_0 = 6.67 \times 10^{-14}\ \text{m}^2$ and $K_0 = 2.69 \times 10^{-7}$ m. The

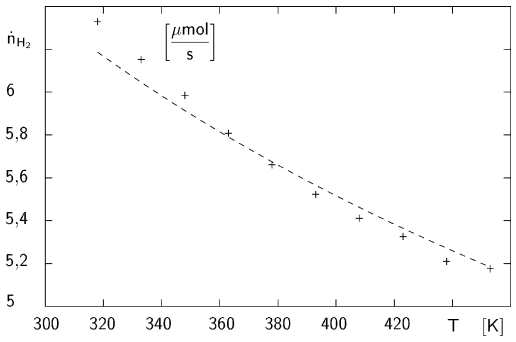

Fig. 5. Steady-state hydrogen flux through an MFI zeolite membrane.

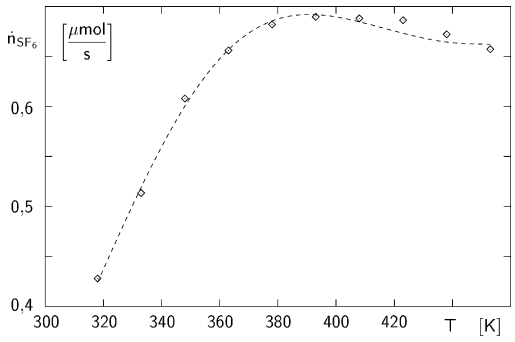

Fig. 6. Sulfur hexafluoride transport through an MFI zeolite membrane.

effective geometrical area A was 2×10^{-4} m^2, the thickness δ was 2.33 mm.

The fitted transport behavior and the experimental results are shown in Fig. 5. The corresponding configuration is more simple than the example shown in Fig. 2. Since surface diffusion was neglected path (b) vanishes. And because there is no activated diffusion process inside the zeolite pores the paths (c) and (d) were merged to a single path of Knudsen diffusion, describing the transport through the zeolitic pores and the grain boundary regions.

The temperature dependence shown almost has a shape corresponding to the assumed Knudsen diffusion mechanism. The value estimated for $\frac{A}{\delta}\frac{\lambda}{z}$ in Eqs. (3), (4) and (9) for $E_{A,GT} = 0$ is 9.624×10^{-11} m^2. There is no visible change if the support resistance is neglected. This is expected. It underlines that for single gas experiments the support influence is negligible and why the Knudsen-like behavior of the temperature dependence of the flux is not strongly distorted by the support resistance.

4.2. Sulfur hexafluoride

As in the treatment of hydrogen, the first question to be answered is the transport mechanism of sulfur hexafluoride in the zeolite pores. Sulfur hexafluoride adsorbs much stronger than hydrogen (but less than the butane isomers, for example), so an important mechanism is surface diffusion. As it is known from literature [3,26], even for the stronger adsorbing hydrocarbons a large amount of desorbed molecules takes part in the permeation. This should be similar for sulfur hexafluoride. Since these molecules are quite bulky (the kinetic diameter of 0.55 nm is well in the range of the diameter of MFI zeolite pores) this diffusion mechanism is presumably activated. For the activation energy a value of 19 kJ mol^{-1} was taken from literature [27].

Similar as in the treatment of hydrogen, to account for possible mesoporous defects in the grain boundary regions an additional non-activated Knudsen transport mechanism was added. The porous support was simulated with the dusty gas model, with the same parameters already applied in the case of hydrogen.

The experimental and the simulated data for the transport of sulfur hexafluoride are shown in Fig. 6. The configuration used for this simulation is the same as shown in Fig. 2. The corresponding parameter estimates are listed in Table 1.

As already observed in the simulation of hydrogen single gas transport, the support resistance has no significant influence on the flux. The calculated parameter estimates for the unary system do not change significantly for sulfur hexafluoride if the support resistance is ignored.

Since the transport mechanism inside the zeolite pores (activated gas diffusion and surface diffusion) differs from the way the molecules permeate through the grain boundary regions (non-activated Knudsen diffusion) it is possible here to quantify the flow through these defects. A breakdown of the different contributions to the total flux is shown in Fig. 7.

It can be seen, that surface diffusion dominates at lower temperatures, while at higher temperatures a comparable amount of molecules is transported according to an activated gas diffusion mechanism. This phenomenon is similar to the transport of hydrocarbons through zeolite membranes [3,26]: at lower temperatures most molecules are adsorbed. From Fig. 7 it is clear that after a short increase of the permeating flow (surface diffusion is also an activated process) with increasing temperature, the amount of adsorbed molecules decreases. Thus, at high temperatures activated gas diffusion dominates. Fig. 7 shows also a very

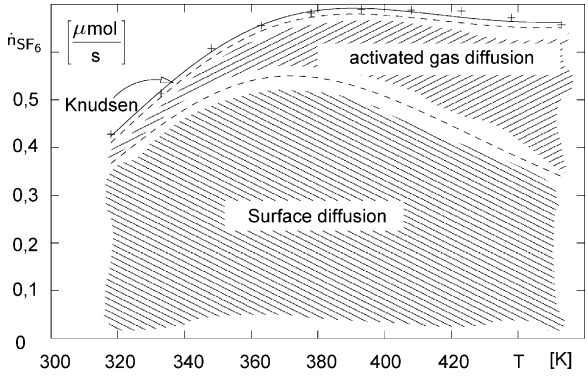

Fig. 7. Contributions of the different transport paths to the total flow.

Table 1
Parameter estimates for simulation of the mass transfer of sulfur hexafluoride through an MFI zeolite membrane

Activated gas diffusion	
(1)	$\frac{A}{\delta}\frac{\lambda}{z} = (6.9 \times 10^{-9} \pm 5 \times 10^{-10})\ \mathrm{m}^2$
	$E_{A,GT} = 19\ \mathrm{kJ\ mol^{-1}}$ [27]
Surface diffusion	
(2)	$\frac{A}{\delta}\rho D^0_{S,0} = (0.16 \pm 0.02)\ \mathrm{g/s}$
(3)	$E_{A,s} = (17.0 \pm 0.5)\ \mathrm{kJ\ mol^{-1}}$
Knudsen diffusion (defects)	
(4)	$\frac{A}{\delta}\frac{\lambda}{z} = (4 \times 10^{-12} \pm 5 \times 10^{-12})\ \mathrm{m}^2$

low contribution of Knudsen diffusion. This indicates, that most of the molecules pass through the zeolitic pores. The defect density of the membrane is small or the defects are so small that the diffusion is activated as well.

4.3. Binary system

Since the simulation of the unary behavior of sulfur hexafluoride gave a small and negligible flow through the grain boundary regions, this transport path was not necessary for the simulation of the binary mass transfer of the system hydrogen/sulfur hexafluoride.

The resulting configuration describes the transport through the porous support via the dusty gas model. The zeolite layer is modelled in terms of two parallel transport paths: one describes the movement of adsorbed molecules by surface diffusion while the other accounts for the permeation of desorbed molecules. Desorbed hydrogen has no activation energy while for sulfur hexafluoride the value of 19 kJ mol^{-1}[27] previously used was maintained. However, this configuration assumes, that there is no interaction between hydrogen and sulfur hexafluoride inside the zeolite pores. It is obvious, that this is only valid for diluted systems.

Because the single gas experiments were carried out without sweep gas, it was important to perform the

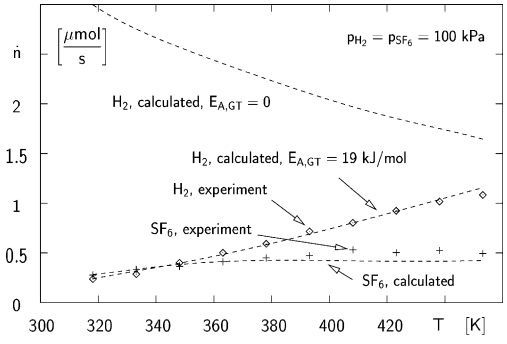

Fig. 8. The binary system hydrogen/sulfur hexafluoride. Observed and modelled molar flows using an equimolar feed.

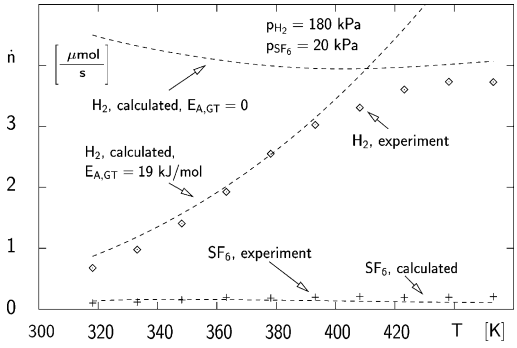

Fig. 9. The binary system hydrogen/sulfur hexafluoride with a molar ratio of 9:1 in the retentate.

experiments on the binary system under the same conditions. Otherwise the counter diffusion of the sweep gas and also the concentration dependency of the diffusion coefficients would not have been taken into account properly.

Figs. 8 and 9 show the results of two different experiments. In the first figure the hydrogen/sulfur hexafluoride mixture on the retentate side is equimolar, while the second figure shows an experiment where the molar ratio of hydrogen to sulfur hexafluoride was 9:1.

In both simulations the flow of sulfur hexafluoride is well predicted while the hydrogen flow is overestimated. The discrepancy is most pronounced for a high concentration of sulfur hexafluoride, as a comparison of Figs. 8 and 9 shows. There is another indication for this phenomenon: at lower temperatures the differences between simulation and experiment for hydrogen are larger. At higher temperatures the prediction of the experimental data is good. This can be explained by the lower surface concentration of sulfur hexafluoride at high temperatures, since the pressure and the volume remain unchanged.

It is quite interesting to see, that hydrogen permeation can be predicted, when the same activation energy as for sulfur hexafluoride (19 kJ mol^{-1}) is used. This observation can be explained by a single file diffusion mechanism. Apparently it is impossible for the faster moving hydrogen molecules to pass the slower sulfur hexafluoride molecules inside the zeolite pores. In other words: the discrepancy between predicted data and experimental data is because the interaction between the two molecules is not taken into account in the model while in reality the two pathways that describe the zeolite layer are not independent.

5. Conclusions

A method that allows the combination of different transport mechanisms for the simulation of the mass transfer inside composite systems is presented. The concept takes the heterogeneous structure of the system into account. It is not restricted to single component systems, and unknown transport parameters can be estimated from

experimental data. So it can serve for the modelling of membrane reactors.

The method was applied to simulate the permeation of hydrogen and sulfur hexafluoride through a flat silicalite-1 zeolite membrane on a porous sinter metal support with a diameter of 18 mm as a model system. The calculated flows of the binary system are based on experimental data of the unary systems. The used model configuration neglects the interactions between hydrogen and sulfur hexafluoride inside the zeolite layer, because of the parallel pathways of surface diffusion and activated gas diffusion. So this oversimplified model is only valid for the diluted system at high temperatures. At low temperatures the calculated hydrogen flow is too high. In reality the pores of the MFI type zeolite are too small to allow the faster hydrogen molecules to pass by the slower sulfur hexafluoride. This effect is less important at higher temperature as the concentration of sulfur hexafluoride decreases and pore blocking reduces.

The discrepancy between experiment and simulation is that strong, because the two molecules of the model system act differently. The tendency of hydrogen and sulfur hexafluoride to adsorb are too different. For two strongly adsorbing species, the problem would most likely not arise. If the transport can be described by a single pathway of multicomponent surface diffusion, the IAS theory can handle the interactions between the different molecules [28].

It must be emphasized that even though it was not possible to predict the gas mixture transport behavior of the examined system correctly, the approach gave some insight concerning the complex nature of the mass transfer inside microporous composite membranes. The simulations show that there is no significant influence of the support layer on the total mass transfer. But this is only valid because during the experiments no sweep gas was used and the permeating flux is not too high. The results also show the way to overcome the discrepancy between experimental and simulated data at lower temperatures. It should be possible to merge the two parallel pathways describing the zeolite layer provided that an appropriate interaction between the two is added.

References

[1] O. Schramm, A. Seidel-Morgenstern, Chem. Eng. Sci. 54 (1999) 1447–1453.
[2] B. Millot, A. Méthivier, H. Jobic, H. Moueddeb, J.-A. Dalmon, Microporous Mesoporous Mater. 38 (2000) 85–95.
[3] W.J. Bakker, L.J.P. van den Broeke, F. Kapteijn, J. Moulijn, AIChE J. 43 (1997) 2203–2214.
[4] S. Farooq, I.A. Karimi, J. Membr. Sci. 186 (2001) 109–121.
[5] U. Beuscher, C.H. Gooding, J. Membr. Sci. 150 (1998) 57–73.
[6] P.H. Nelson, M. Tsapatsis, S.M. Auerbach, J. Membr. Sci. 184 (2001) 245–255.
[7] F. Jareman, J. Hedlund, D. Creaser, J. Sterte, J. Membr. Sci. 236 (2004) 81–89.
[8] E.A. Mason, A.P. Malinauskas, Gas Transport in Porous Media: The Dusty-Gas Model, Elsevier, Amsterdam, 1983.
[9] E.A. Mason, A.P. Malinauskas, R.B. Evans III, J. Chem. Phys. 46 (1967) 3199–3216.
[10] J. Xiao, J. Wei, Chem. Eng. Sci. 47 (1992) 1123–1141.
[11] R. Krishna, Gas Sep. Purif. 7 (1993) 91–104.
[12] F. Kapteijn, J.A. Moulijn, R. Krishna, Chem. Eng. Sci. 55 (2000) 2923–2930.
[13] A.L. Myers, J.M. Prausnitz, AIChE J. 11 (1965) 121–127.
[14] E. Buß, Chem. Technik 48 (1995) 189–197.
[15] R. Schöllner, T. Franke, P. Mahn, G. Kluge, Chem. Technik 45 (1993) 453–460.
[16] M.D. LeVan, T. Vermeulen, J. Phys. Chem. 85 (1981) 3247–3250.
[17] H. Moon, C. Tien, Ind. Eng. Chem. Res. 26 (1987) 2042–2047.
[18] J.A. O'Brien, A.L. Myers, Ind. Eng. Chem. Res. 27 (1988) 2085–2092.
[19] W.H. Press, S.A. Teukolsky, W.T. Vetterling, B.P. Flannery, Numerical Recipes in C, Cambridge University Press, Cambridge, 1999.
[20] G.T.P. Mabande, W. Schwieger, M. Hanebuth, R. Dittmeyer, T. Selvam, in: E. van Steen, L.H. Callanan, M. Clays (Eds.), Proceedings of the 14th International Zeolite Conference, Cape Town, South Africa, 2004, pp. 695–702.
[21] M. Hanebuth, R. Dittmeyer, G.T.P. Mabande, W. Schwieger, Chem. Ing. Tech. 75 (2003) 221–227.
[22] P. Ciavarella, H. Moueddeb, S. Miachon, K. Fiaty, J.-A. Dalmon, Catal. Today 56 (2000) 253–264.
[23] C. Bai, M. Jia, J.L. Falconer, R.D. Noble, J. Membr. Sci. 105 (1995) 79–87.
[24] Y. Takata, T. Tsuru, T. Yoshioka, M. Asaeda, Microporous Mesoporous Mater. 54 (2002) 257–268.
[25] T.C. Golden, S. Sircar, J. Colloid Interface Sci. 162 (1994) 182–188.
[26] F. Kapteijn, J.M. van de Graaf, J.A. Moulijn, AIChE J. 46 (2000) 1096–1100.
[27] H. MacDougall, D.M. Ruthven, Adsorption 5 (1999) 369–372.
[28] L.J.P. van den Broeke, W.J.W. Bakker, F. Kapteijn, J.A. Moulijn, AIChE J. 45 (1999) 976–985.